Pedal to Pavement: An Energy-Based Proper Vehicle Model

Greg Browne[#1], Nicholas Krouglicof[#2]

[#]*Faculty of Engineering and Applied Science, Memorial University*
St. John's, Newfoundland A1B 3X5 Canada

[1]g.browne@mun.ca

[2]nickk@mun.ca

Abstract— **Partial and complete vehicle models are an essential element of the design process within the automotive industry.**

This paper constructs an energy-based (bond graph) proper model of a complete vehicle. This model includes all significant system dynamics generated from pressing on the gas pedal to the resulting vehicle translation.

A complete model, containing 65 elements, is reduced via the Model Order Reduction Algorithm (MORA) to one that contains 22 elements, provides simulation results of adequate agreement, and still contains over 98% of the original system energy.

The proper model reduces the number of calculations by 86% and the simulation time by 92%. The proposed model and modeling techniques presented in this paper could greatly improve the efficiency of automotive simulation and design.

***Keywords*— bond graph modeling, model simulation, reduced order systems, road vehicle modeling, spark ignition engine modeling**

I. INTRODUCTION

Partial and complete vehicle models are an essential element of the design process within the automotive industry. Due to the prevalence of model-based design in this industry, a proper model of a complete vehicle can improve the efficiency of, at least, one stage of the design cycle.

Bond graphs are an efficient way of describing multiport systems in that the connections (bonds) between system elements have both an effort and a flow whose product is the power of the bond [1]. Moreover, bond graphs allow for the seamless interconnection of systems across energy domains (hydraulics, rotational mechanics, translational mechanics, electrodynamics, etc). Therefore, bond graphs are used as the preferred means of modeling presented in this paper. For more details on bond graphs refer to [1].

In order for a complete vehicle model to suitably describe all significant system dynamics generated from pressing on the gas pedal to the resulting vehicle translation, it should suitably describe each of the major vehicle systems:

1. Fuel Delivery System
2. Air Induction System
3. Powertrain
4. Suspension

These systems are illustrated in the vehicle system cutaway in Fig. 1, and are described in detail in the following sections.

Fig. 1. Vehicle Cutaway (courtesy of *CanadianDriver Communications Inc*.)

II. MODEL CONSTRUCTION

A. Fuel Delivery System

The fuel delivery system pumps fuel from the fuel tank to the engine bay where it is atomized and sprayed by the fuel injectors. The model construction, reduction, and simulation of the fuel delivery system were detailed by the authors in [2].

B. Air Induction System

The air induction system measures and controls the air flow from the atmosphere to the engine cylinders.

1) Throttle Body

The throttle body allows air to pass from the atmosphere into the intake manifold. Its basis is a throttle (butterfly) valve which controls the amount of air allowed to enter. The mass airflow through the throttle body, $\dot{m}_{TB}$, can be expressed as choked flow through a converging nozzle, as given by (1) [3].

$$\dot{m}_{TB} = \begin{cases} \frac{C_D A_{TB} P_a}{\sqrt{R_{air} T_a}} \left(\frac{P_{man}}{P_a}\right)^{\frac{1}{\gamma}} \sqrt{\frac{2\gamma}{\gamma-1}\left[1-\left(\frac{P_{man}}{P_a}\right)^{\frac{\gamma-1}{\gamma}}\right]}, \frac{P_{man}}{P_a} < \mathrm{P_c} \\ \frac{C_D A_{TB} P_a}{\sqrt{R_{air} T_a}} \gamma^{\frac{1}{2}} \left(\frac{2}{\gamma+1}\right)^{\frac{\gamma+1}{2(\gamma-1)}}, \text{otherwise} \end{cases} \quad (1)$$

Where, C_D is the discharge coefficient of the throttle valve, A_{TB} is the effective area through which air may flow, P_a and T_a are the ambient pressure and temperature respectively, R_{air}

and γ are the gas constant and adiabatic index specific to dry air respectively, P_{man} is the manifold pressure, and P_c is the critical pressure, above which the flow is choked.

The effective area, A_{TB}, can be approximated as the area of two circle segments created by the projection of the throttle valve onto the cross-section of the throttle body. This area is given by (2).

$$A_{TB} = \frac{D^2}{2}\left[\cos^{-1}\left\{\frac{\cos(\alpha+\alpha_c)}{\cos\alpha_c}\right\} - \frac{\cos(\alpha+\alpha_c)}{\cos\alpha_c}\sqrt{1-\left[\frac{\cos(\alpha+\alpha_c)}{\cos\alpha_c}\right]^2}\right]$$
(2)

Where, D is the throttle body diameter, α is the variable angle by which the throttle is opened, and α_c is the throttle angle when it is fully closed. These parameters are illustrated in Fig. 2.

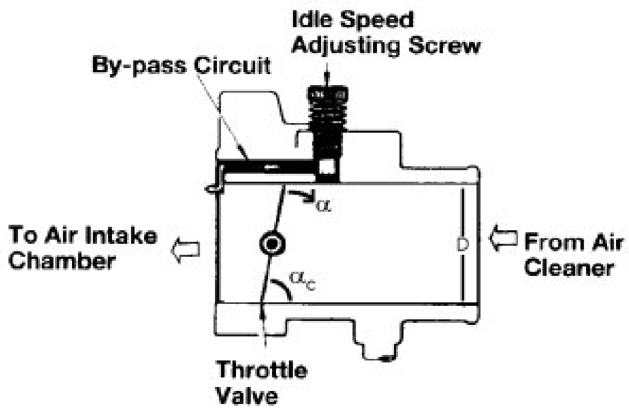

Fig. 2. Throttle Body Side View (based on image courtesy of Toyota Motor Sales)

The bond graph form of the throttle body submodel is illustrated in Fig. 3.

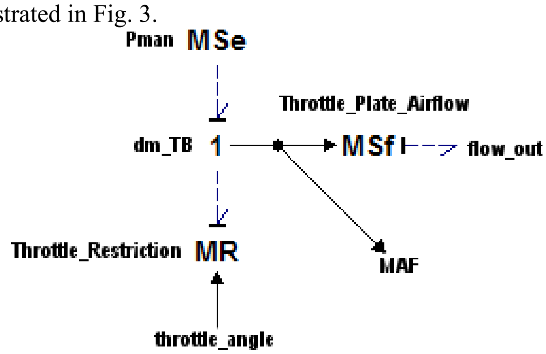

Fig. 3. Throttle Body Submodel

2) Intake Manifold

The intake manifold distributes the delivered air through its runners to the engine cylinders. The manifold pressure, which directly affects most subsystems in the fuel delivery and air inductions system, is given by the ideal gas law, (3).

$$P_{man} = \left(m_{TB} - \sum m_{c,i}\right)\frac{R_{air}T_{man}}{V_{man}} \quad (3)$$

Where, $m_{c,i}$ is the air mass entering cylinder *i*, T_{man} and V_{man} are the temperature and volume of the manifold respectively.

This relationship, for a 4-cylinder engine, is given in bond graph form in Fig. 4.

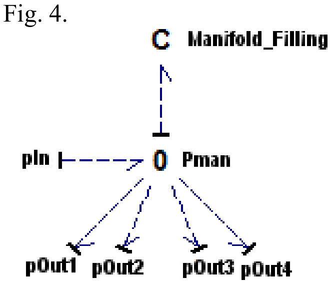

Fig. 4. Intake Manifold Submodel

3) Cylinders

During the *intake stroke*, the intake valve is open and the cylinder in question is filled with the air-fuel mixture provided by the intake manifold runner and fuel injector. The mass airflow into a given cylinder, $\dot{m}_c$, is given by (4).

$$\dot{m}_c = \frac{P_{man}}{R_{air}T_{man}}\left(\frac{V_d}{2n_c}\right)\left(\frac{\omega_c}{2\pi}\right) \quad (4)$$

Where, V_d is the total engine displacement, n_c is the number of cylinders, and ω_c is the angular speed of the crankshaft.

Furthermore, during the *power stroke*, the air-fuel mixture undergoes combustion, whereby its mass is converted into energy, E_c, as given by (5).

$$E_c = \left(\frac{\dot{m}_c}{\omega_c}\right)H_u\eta_i \quad (5)$$

Where, H_u is the heating value of the fuel and η_i is the indicated efficiency, given by the experimental equation, (6) [4].

$$\eta_i = 0.558(1 - 2.092\omega_c^{-0.36}) - 0.015 \quad (6)$$

These dynamics are represented as bond graphs in Fig. 5.

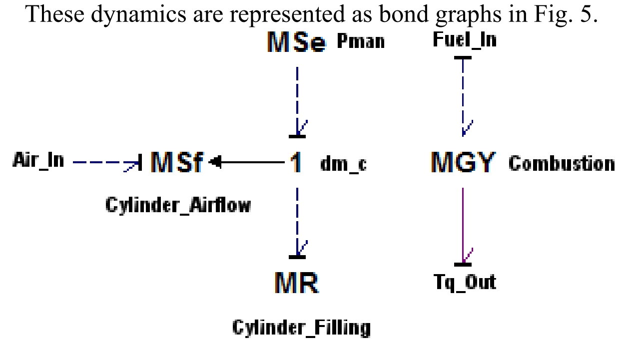

Fig. 5. Cylinder Submodel

C. Powertrain

The powertrain consists of the system components that convert the energy from combustion into kinetic energy (i.e. movement).

1) Crankshaft

The crankshaft is driven by each piston during the *power stroke*, which effectively converts the combustion energy into a torque, τ_{in}. The crankshaft speed, ω_c, directly affects the fuel delivery and air induction systems, while the effective torque provided by the crankshaft, τ_{out}, affects the rest of the powertrain. These quantities are related via (7).

$$\omega_c = \frac{1}{I_{eff}} \int \left(\tau_{in} - \tau_f - \tau_{out}\right) dt \tag{7}$$

Where, I_{eff} is the effective inertia as seen by the crankshaft and τ_f is the loss due to friction, which encompasses pumping losses during intake and exhaust strokes, rubbing friction between adjacent engine components, and losses associated with driving essential engine accessories. Furthermore, I_{eff} is given by (8), τ_f is calculated using the friction correlation, (9), adapted from [3], and τ_{out} is approximated as a parabola with a peak at the max indicated torque, τ_{max}, and passes through the max indicated power, P_{max}, at the indicated crankshaft speeds (ω_τ and ω_P), as shown in (10).

$$I_{eff} = I_e + I_t + \frac{I_d + (4m_w + m_v + m_p)(r_w/R_{FD})^2}{R_G^2} \tag{8}$$

$$\tau_f = \frac{V_d}{4\pi}\left(0.456\omega_c^2 + 143.24\omega_c + 9.7 \times 10^4\right) \tag{9}$$

$$\tau_{out} = \tau_{max} - \left(\tau_{max} - \frac{P_{max}}{\omega_P}\right)\left(\frac{\omega_c - \omega_\tau}{\omega_P - \omega_\tau}\right)^2 \tag{10}$$

Where, I_e, I_t, and I_d are the engine, transmission, and driveshaft inertias respectively, m_w, m_v, and m_p are the wheel, vehicle, and passenger(s) masses respectively, r_w is the wheel radius, R_{FD} and R_G are the final drive and (active) gear ratios respectively (described in the following sections).

The crankshaft dynamics are given in bond graph form in Fig. 6.

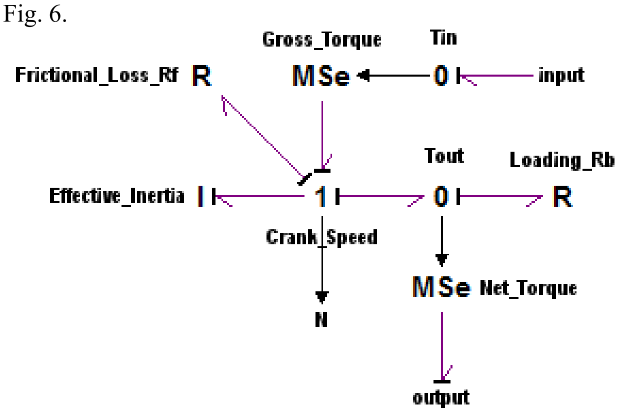

Fig. 6. Crankshaft Submodel

2) Gearbox

The output torque from the crankshaft is applied to the input shaft of the gearbox. It contains a planetary gear / sun gear assembly which provide multiple discrete (for traditional transmissions) forward gear ratios, R_G, and a reverse gear ratio. Low gears are used to generate the higher torque required for getting the vehicle up to speed [5] while high (and overdrive) gears are used to improve efficiency at high speeds.

Gear selection is executed via a signal from the vehicle's Powertrain Control Module (PCM) or standalone Transmission Control Unit (TCU). The PCM/TCU uses data from the vehicle speed sensor and throttle position sensor as indices in a 2D lookup table or *shift schedule*, to determine in which gear the gearbox should be.

Furthermore, the input and output shafts of the gearbox have an associated stiffness and damping which affects their rotation.

The gearbox submodel is illustrated in bond graph form in Fig. 7.

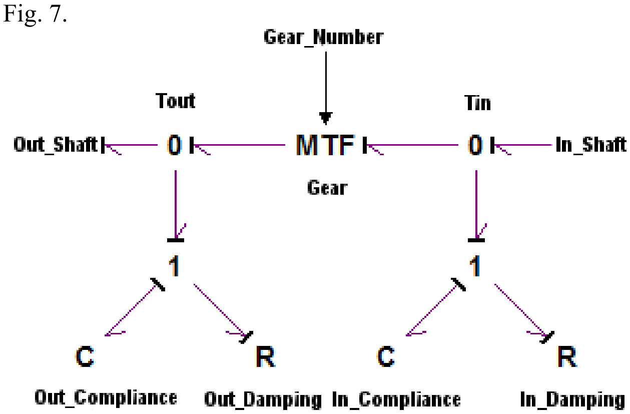

Fig. 7. Gearbox Submodel

3) Differential

The differential takes the transverse rotation of the gearbox output shaft and converts it to longitudinal rotation, in order to drive the wheels.

Another torque multiplication is applied via the final drive ratio, R_{FD}, before being applied (in equal amounts) to the driven wheels. Moreover, the wheels are permitted to rotate at different speeds to facilitate maneuvering [6].

The differential submodel is shown in bond graph form in Fig. 8.

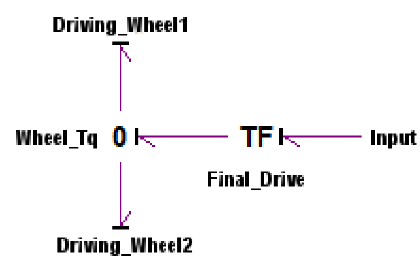

Fig. 8. Differential Submodel

4) Wheels

The torque applied to the wheel by the differential, τ_w, is converted to a tractive force, F_T, which causes the vehicle to move. This relationship is given by (11).

$$F_T = \frac{\tau_w}{r_w} - F_L \tag{11}$$

Where, F_L is the loss due to rolling resistance. For the non-driven wheels, $\tau_w = 0$.

The wheel submodel is shown in bond graph form in Fig. 9.

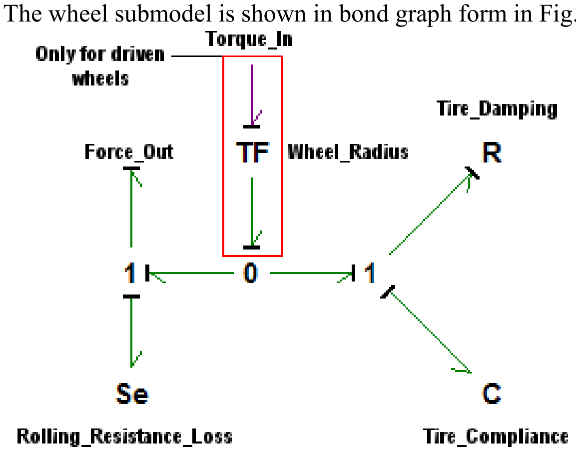

Fig. 9. Wheel Submodel

The resulting speed of the vehicle, v_v, can be determined by accumulating the forces acting upon the vehicle, and applying Newton's 2nd law, as given by (12).

$$v_v = \int \frac{\sum F_{T,i} - F_D - F_R}{m_v + m_p} dt \tag{12}$$

Where, F_D is the aerodynamic drag given by (13) [7] and F_R is the loading due to the road profile, given by (14).

$$F_D = \tfrac{1}{2} C_d \rho_{air} A_F v_v^2 \tag{13}$$

$$F_R = \left(m_v + m_p\right) g \sin\theta_R \tag{14}$$

Where, C_d is drag coefficient, ρ_{air} is the density of air, A_F is the vehicle frontal area, g is the acceleration due to gravity, and θ_R is the angle of inclination of the road.

D. Suspension

The function of a vehicle's suspension is to either provide suitable ride quality (e.g. by smoothing out bumps in the road), improved handling (e.g. tight cornering), or some compromise between the two.

1) Struts

Typically, struts consists of a coil spring to support the vehicle's weight, a strut housing to provide rigid structural support for the assembly, and a damping unit within the strut housing to control spring and suspension movement [8].

The bond graph representation of a strut is given in Fig. 10.

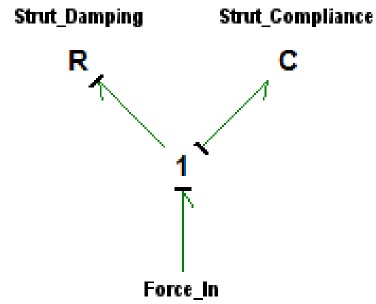

Fig. 10. Strut Submodel

Furthermore, if the vehicle utilizes shock absorbers instead of struts, on two or four of the corners of the vehicle, the bond graph model is the same, but the element values are different.

2) Tires

The tires also act as a stiff spring to support the weight of the vehicle.

The bond graph representation of each tire was given previously with the wheel submodel in Fig. 9.

E. Submodel Interconnection

Due to the nature of bond graphs, the submodels can be easily interconnected to form the complete vehicle model.

III. Model Reduction

By utilizing a method that quantizes the contribution of each element, one can make an informed decision regarding which elements to retain and which to eliminate from a proper model. A proper model has minimal complexity, physically meaningful parameters, and accurately predicts dynamic system responses [9].

The Model Order Reduction Algorithm (MORA) uses activity, A_i, to quantize the contribution of a given element. Activity is "absolute energy" and, for a given element *i*, is calculated by (15) [9].

$$A_i = \int |P_i(t)|\, dt \tag{15}$$

Where, P_i is the instantaneous power of element *i*.

Each element is assigned a non-dimensional activity index, AI_i, which is its fraction of the total system activity. For a given element *i* of *k* elements, its activity index is calculated using (16) [9].

$$AI_i = \frac{A_i}{A_{Total}} = \frac{\int |P_i(t)|\, dt}{\sum_{i=1}^{k}\{\int |P_i(t)|\, dt\}} \tag{16}$$

Activity indices are then sorted and elements eliminated from the lower end until the minimum number of elements required to satisfactorily reproduce the responses of the complete model is achieved.

A. Element Elimination

In order to properly exercise the model, three 30-second simulation profiles were executed to acquire activity data:

1. Full throttle, flat road
2. 50% throttle, 15° inclined road
3. Variable throttle, 1° inclined road

In the following discussion, *Profile 3* (variable throttle) will be used for illustration, and its activity analysis is given in Appendix A.

By following the MORA, the following 43 of 65 submodel elements can be eliminated and still produce simulation results with reasonable agreement to the complete model:

1) Fuel Delivery System

- Pressure Regulator submodel
- Return and Fuel Pipe submodels
- Resistances, inertias, and compressibilities (Fuel Rail submodel)
- Leakage coefficient (Fuel Pump submodel)

2) Powertrain

- Damping and compliances (Gearbox submodel)
- Driveshaft, engine inertias, and wheel mass (Crankshaft submodel)

3) Suspension

- Damping and compliances (Wheel and Strut submodels)

If the MORA were to be strictly followed, the following would also have been eliminated:

- Needle valves (Injector submodels)
- Spring compliance (Pulsation Damper submodel)
- Manifold filling (Intake Manifold submodel)
- Cylinder filling (Cylinder submodels)

However, these submodel elements were retained because of their physical meaningfulness. While the elements may not be active in terms of their power or energy, they provide important signals to be used by other parts of the model.

The injector needle valves provide the discretized fuel packets which provide the energy for the powertrain (via combustion).

The pulsation damper spring compliance (or stiffness) determines the fuel rail pressure used for fuel injection.

The manifold and cylinder filling determines (in conjunction with the throttle body submodel) the manifold pressure used throughout the fuel delivery and air induction systems.

B. Reduced Model Validation

Model outputs for the application presented in this paper are manifold pressure, P_{man}, crank speed, ω_c, and vehicle speed, v_v. The simulation results for these quantities for the complete and reduced models are compared in Fig. 11-13.

One can see that the simulation results from reduced model follow the complete model relatively well. Based on the given application, the agreement is considered adequate.

The complexity of the complete model, shown in Appendix B, and reduced model, shown in Appendix C, can also be easily compared by observing the model structure.

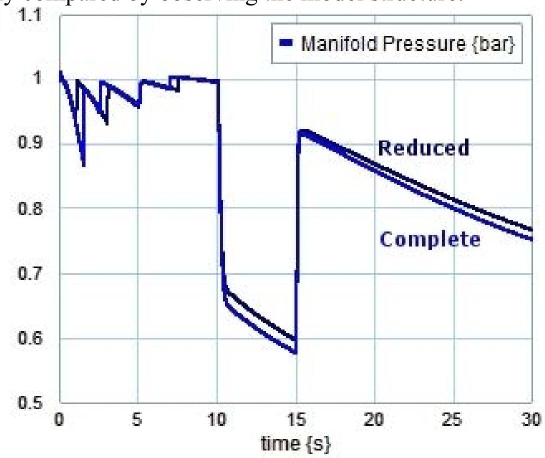

Fig. 11. Manifold Pressure Curves for Complete and Reduced Models

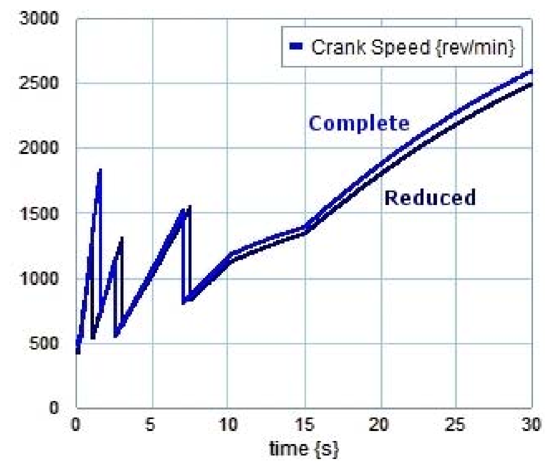

Fig. 12. Crank Speed Curves for Complete and Reduced Models

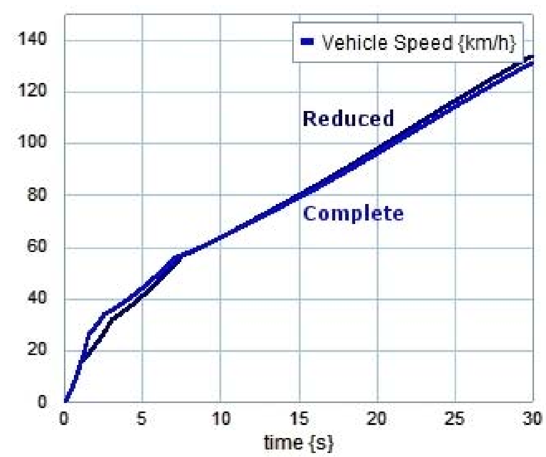

Fig. 13. Vehicle Speed Curves for Complete and Reduced Models

IV. Conclusion

The reduced model presented in this paper consists of the 22 most active of 65 elements, yet still provides simulation results of adequate agreement to the complete model. By eliminating 43 elements, model calculations were reduced from an average of 3 041 653 to 437 960 (about 86%) for 30 seconds of simulation. Furthermore, simulation time was reduced from an average of 142 seconds to 12 seconds (about 92%). It is also important to note that the reduced model still retained over 98% of the original system activity.

Moreover, any further attempt to eliminate system elements resulted in large simulation deviations from those of the complete model. These deviations were most prominent when they caused the automatic transmission to change gears at a time other than that of the complete model.

The definition of "adequate agreement" obviously depends on the application. The application presented in this paper considers throttle angle and road profile to be the inputs and manifold pressure, crank speed, and vehicle speed to be the outputs. However, if one was interested in studying ride quality, throttle angle and road profile might still be the inputs, but the most important output may be strut displacement, for example. Therefore, more elements may need to be retained (the reduced model presented eliminated the entire suspension system) or *different* elements may be able to be eliminated and still provide results for that application's "adequate agreement".

The implication of the material presented in the paper is reflected in improving the efficiency of model-based design by reducing simulation time and model complexity. Furthermore, such models as the one presented can be used to predict vehicle characteristics such as fuel economy and performance (e.g. 0-60 and quarter-mile times).

Beyond reducing the computational complexity, the submodels of the system could also be imploded into iconic sections for easier analysis, as illustrated in Appendix D.

Appendix

A. Activity Analysis for Variable Throttle, 1° Inclined Road

TABLE I

Activity Analysis for Variable Throttle, 1° Inclined Road

Submodel	Element	Activity Index	Cumulative Activity
Crankshaft	Vehicle Mass	34.4526%	34.45265%
Crankshaft	Loading	22.7763%	57.22896%
Drag	Drag	15.7735%	73.00246%
Road Load	Road Load	5.57442%	78.57688%
Crankshaft	Friction	3.98841%	82.56529%
LF Wheel	Rolling Resistance	2.47175%	85.03704%
RF Wheel	Rolling Resistance	2.47175%	87.50880%
Throttle Body	Throttle Restriction	2.04651%	89.55531%
Crankshaft	Passenger Mass	1.87514%	91.43045%
LR Wheel	Rolling Resistance	1.84024%	93.27069%
RR Wheel	Rolling Resistance	1.84024%	95.11093%
Crankshaft	Transmission Inertia	1.19435%	96.30528%
Crankshaft	Wheel Mass	0.85007%	97.15534%
Cyl1	*Cylinder Filling*	*0.51199%*	*97.66733%*
Cyl2	*Cylinder Filling*	*0.51199%*	*98.17933%*
Cyl3	*Cylinder Filling*	*0.51199%*	*98.69132%*
Cyl4	*Cylinder Filling*	*0.51199%*	*99.20331%*
Crankshaft	Engine Inertia	0.47774%	99.68105%
Crankshaft	Driveshaft Inertia	0.23039%	99.91144%
LF Strut	Strut Compliance	0.01717%	99.92861%
RF Strut	Strut Compliance	0.01717%	99.94578%
Manifold	*Manifold Filling*	*0.00724%*	*99.95303%*
LF Strut	Strut Damping	0.00668%	99.95970%
RF Strut	Strut Damping	0.00668%	99.96638%
Pressure Reg	Orifice Restriction	0.00533%	99.97171%
Fuel Pump	Pump Loss	0.00504%	99.97675%
LF Wheel	Tire Compliance	0.00484%	99.98159%
RF Wheel	Tire Compliance	0.00484%	99.98643%
P Damper	*Spring Compliance*	*0.00314%*	*99.98957%*
LF Wheel	Tire Damping	0.00139%	99.99096%
RF Wheel	Tire Damping	0.00139%	99.99235%
Fuel Rail	Rail Inertia3	0.00115%	99.99349%
Fuel Rail	Rail Inertia1	0.00115%	99.99464%
Fuel Rail	Fuel Compress1	0.00093%	99.99557%
Fuel Rail	Fuel Compress2	0.00093%	99.99651%
Return Pipe	Return Pipe Inertia	0.00082%	99.99733%
Fuel Rail	Rail Inertia2	0.00075%	99.99808%
Return Pipe	Fuel Compress	0.00059%	99.99867%
Fuel Rail	Fuel Compress3	0.00032%	99.99899%
Inj1	*Needle Valve*	*0.00016%*	*99.99915%*
Inj4	*Needle Valve*	*0.00016%*	*99.99931%*
Inj3	*Needle Valve*	*0.00016%*	*99.99947%*
Pressure Reg	Regulator Mass	0.00008%	99.99955%
Inj2	*Needle Valve*	*0.00008%*	*99.99963%*
Gearbox	In Compliance	0.00007%	99.99970%
Fuel Pipe	Fuel Pipe Resist	0.00005%	99.99975%
Return Pipe	Return Pipe Resist	0.00004%	99.99979%
Pressure Reg	Spring Compliance	0.00004%	99.99982%
Fuel Rail	Rail Resistance1	0.00003%	99.99985%
Fuel Rail	Rail Resistance2	0.00003%	99.99988%
Fuel Rail	Rail Resistance3	0.00003%	99.99991%
Gearbox	Out Compliance	0.00002%	99.99994%
Fuel Pipe	Fuel Compress	0.00002%	99.99996%
Fuel Pipe	Fuel Pipe Inertia	0.00001%	99.99997%
Gearbox	In Damping	0.00001%	99.99998%
Pressure Reg	Fuel Damping	0.00001%	99.99999%
Gearbox	Out Damping	0.00001%	100.00000%
LR Strut	Strut Damping	0.00000%	100.00000%
RR Strut	Strut Damping	0.00000%	100.00000%
LR Wheel	Tire Compliance	0.00000%	100.00000%
RR Wheel	Tire Compliance	0.00000%	100.00000%
LR Strut	Strut Compliance	0.00000%	100.00000%
RR Strut	Strut Compliance	0.00000%	100.00000%
LR Wheel	Tire Damping	0.00000%	100.00000%
RR Wheel	Tire Damping	0.00000%	100.00000%

Elements in grayed-out cells were eliminated during the MORA process.

Elements in italics should have been eliminated by MORA but were retained for their physical significance to the model.

B. Complete Vehicle Model

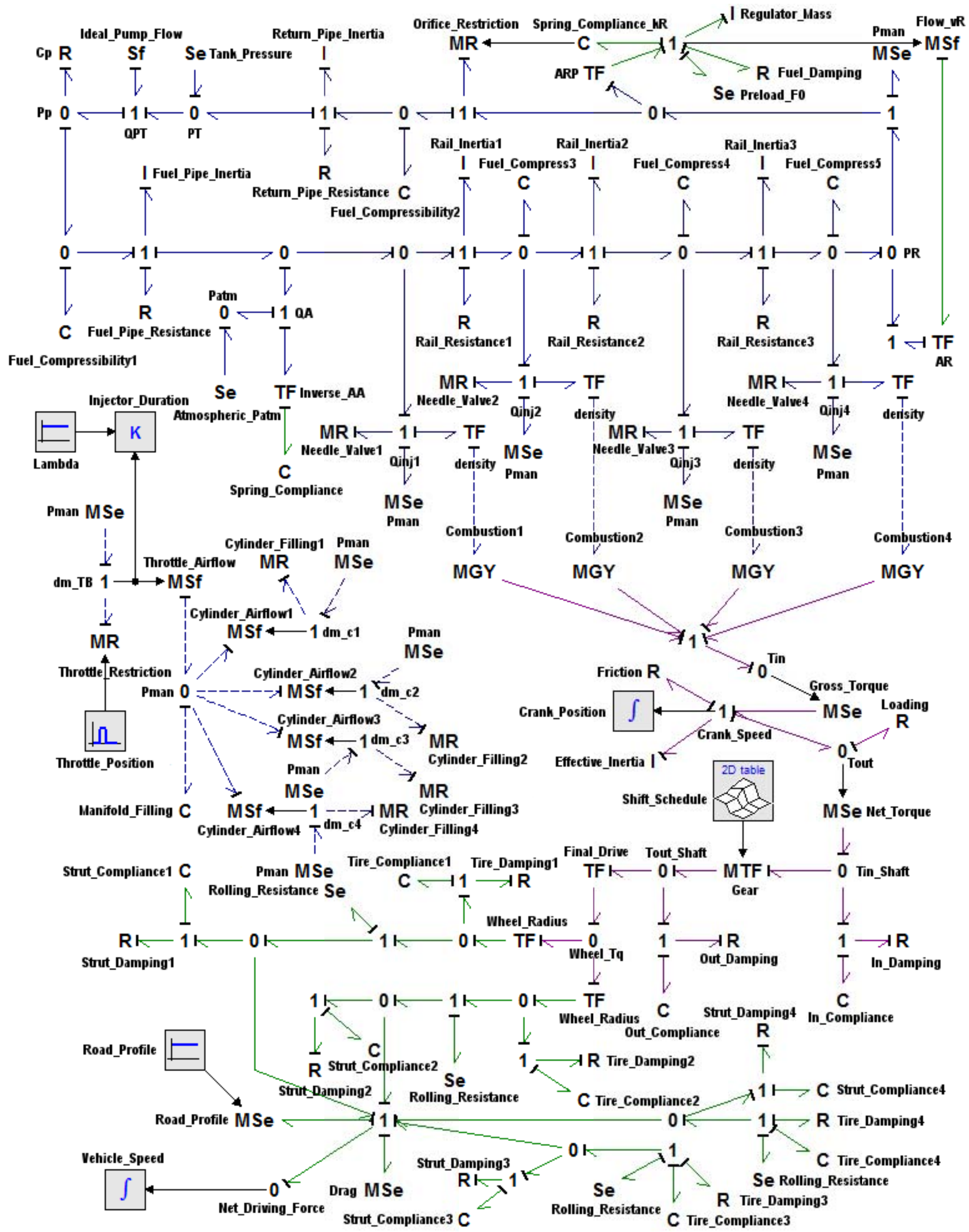

Fig. 14. Complete Vehicle Model

C. Reduced Vehicle Model

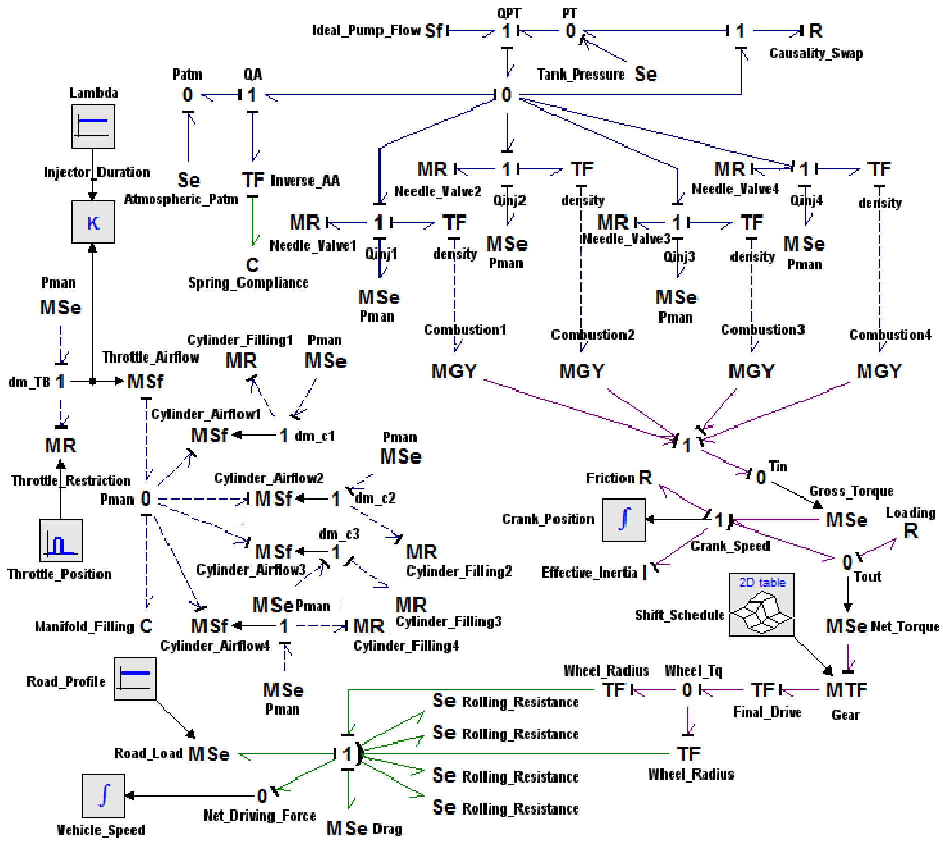

Fig. 15. Reduced Vehicle Model

D. Iconic Vehicle Model

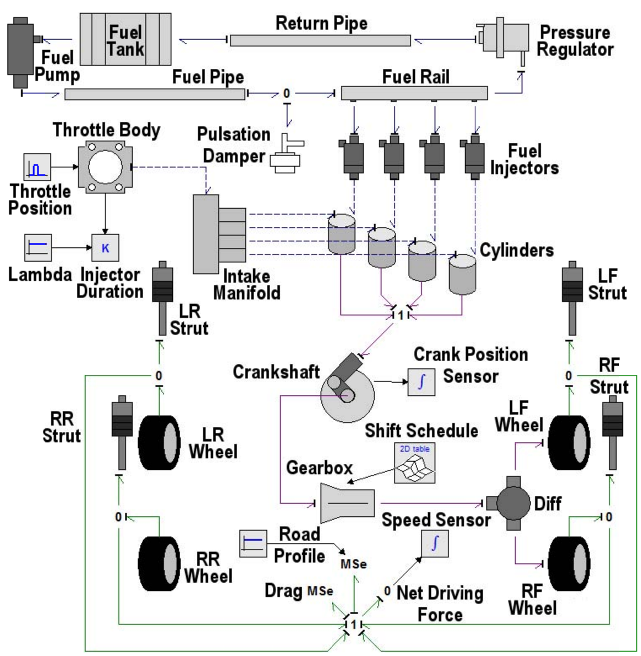

Fig. 16. Iconic Vehicle Model

REFERENCES

[1] Dean C. Karnopp, Donald L. Margolis, and Ronald C. Rosenberg, *System Dynamics - Modeling and Simulation of Mechatronic Systems*, 3rd Ed. New York: Wiley-Interscience, 2000.

[2] Greg Browne, Nicholas Krouglicof, and Geoff Rideout, "An Energy-Based Proper Model of an Automotive Fuel Delivery System," in *Reliability and Robust Design in Automotive Engineering, 2010*, SAE International, 2010.

[3] John B. Heywood, *Internal Combustion Engine Fundamentals*. New York: McGraw-Hill, Inc., 1988, pp. 307, 722.

[4] Elbert Hendricks, Donn Engler , and Marco Fam , "A Generic Mean Value Engine Model for Spark Ignition Engines," in *41st Simulation Conference*, 2000.

[5] Toyota Motor Sales. (2007, Mar.). Gear Selection and Function.

[6] Driving Fast. Differentials. [Online] Available: http://www.drivingfast.net/technology/differentials.htm

[7] Glenn Research Center, NASA. The Drag Equation. [Online] Available: http://www.grc.nasa.gov/WWW/K-12/airplane/drageq.html

[8] Monroe Shocks & Struts. (2008). Struts. [Online]. Available: http://www.monroe.com/support/tec_struts.asp

[9] Loucas S. Louca, Geoff Rideout, Jeffrey L. Stein, Gregory M. Hulbert, "Generating Proper Dynamic Models for Truck Mobility and Handling," *International Journal of Heavy Vehicle Systems*, pp. 1,4, Dec 29, 2003.